

Supporting Information

For

Triple Targeting Host-guest Drug Delivery System Based on Lactose-Modified Azocalix[4]arene for Tumor Ablation

Juan-Juan Li,^{‡a} Rui-Xue Rong,^{‡b} Yan Yang,^b Zong-Ying Hu,^a Bing Hu,^c Ying-Ying Zhao,^c Hua-Bin Li,^a Xin-Yue Hu,^{*a} Ke-Rang Wang^{*c} and Dong-Sheng Guo^{*a}

^a College of Chemistry, Key Laboratory of Functional Polymer Materials (Ministry of Education), State Key Laboratory of Elemento-Organic Chemistry, Collaborative Innovation Center of Chemical Science and Engineering, Nankai University, Tianjin 300071, China.

^b Department of Medical Microbiology and Immunology, School of Basic Medical Science, Key Laboratory of Medicinal Chemistry and Molecular Diagnosis (Ministry of Education), Key Laboratory of Chemical Biology of Hebei Province, Medical Comprehensive Experimental Center, Hebei University, Baoding 071002, China.

^c College of Chemistry and Environmental Science, Key Laboratory of Medicinal Chemistry and Molecular Diagnosis (Ministry of Education), Key Laboratory of Chemical Biology of Hebei Province, Hebei University, Baoding 071002, China.

*E-mail: huxinyue@nankai.edu.cn

*E-mail: kerangwang@hbu.edu.cn

*E-mail: dshguo@nankai.edu.cn

‡ These authors contributed equally.

Table contents

1 Materials and general methods.....	4
1.1 Materials.	4
1.2 Samples.	4
1.3 Apparatus.	4
1.4 Data analyses of fluorescence titrations.	5
1.5 Fluorescence responses of DOX@LacAC4A and CY5-DM@LacAC4A upon the addition of various biologically coexisting species.	5
1.6 Cytotoxicity Assays <i>in vitro</i>	6
1.7 Cellular internalization analysis.	6
1.8 <i>In vivo</i> fluorescence imaging.	7
1.9 <i>In vivo</i> antitumor efficacy study.	7
1.10 Statistical analysis.	8
2 Syntheses of LacAC4A	8
3 Supporting results and experimental raw data	11
3.1 Job's plot for the complexation of DOX with LacAC4A.	11
3.2 Morphology and stability Evaluation of DOX@LacAC4A.	12
3.3 The binding affinity of DOX with SAC4A.	12
3.4 Cell viabilities of HepG2 cells.	12
3.5 Internalization pathway of LacAC4A.	13
3.6 The binding affinity of CY5-DM with LacAC4A.	13
3.7 Evaluation of the CY5-DM@LacAC4A stability.	14
3.8 <i>Ex vivo</i> fluorescence imaging of tumors and major organs.	14
3.9 Safety evaluation of supramolecular carrier LacAC4A.	15
3.10 Evaluation of the LacAC4A biocompatibility.	17

3.11 H&E stains of the major organs.	18
4 References	19

1 Materials and general methods

1.1 Materials. All the reagents and solvents were commercially available and used as received unless otherwise specified purification. Sodium hyposulfite (SDT) was purchased from J&K Chemical. 4-Aminobenzoic acid, sodium nitrite and rhodamine B (RhB) were purchased from Aladdin. 1,1',3,3',3'-Hexamethylindodicarbocyanine (CY5-DM) was obtained OKeanos Tech. Co.,Ltd. 2-(7-Azabenzotriazol-1-yl)-*N,N,N',N'*-tetramethyluronium hexafluorophosphate (HATU), *N,N*-diisopropylethylamine (DIPEA), propargulamine, copper sulfate pentahydrate ($\text{CuSO}_4 \cdot 5\text{H}_2\text{O}$), sodium ascorbate and sodium methanolate (CH_3ONa) were purchased from TCI. 5,11,17,23-Tetrakis[*(p*-carboxy-phenyl)azo]-25,26,27,28-tetra-hydroxy calix[4]arene (CAC4A) was synthesized according to the previous literature.^{1, 2} Doxorubicin (DOX) was purchased from Energy Chemical. Fetal bovine serum (FBS) and dulbecco's modified eagle medium (DMEM) were purchased from Thermo Fisher Scientific. Cell counting kit-8 (CCK-8) was obtained from Dojindo. Human cervical cancer (Hela) cells, human hepatoma (HepG2) cells and hepatoma 22 (H22) cells were purchased from Procell Life Science&Technology Co.,Ltd.

1.2 Samples. The phosphate buffered saline (PBS) solution of pH = 7.4 was prepared by dissolving 0.603 g of sodium phosphate monobasic dehydrate, 0.870 g disodium phosphate, 8.006 g sodium chloride and 0.201 g potassium chloride in approximate 900 mL double-distilled water. Titrate to pH = 7.4 at the lab temperature of 25 °C with NaOH and make up volume to 1000 mL with double-distilled water. The pH value of the buffer solution was then verified on a pH-meter calibrated with three standard buffer solutions. LacAC4A nanoparticles were prepared by dissolving the solids in PBS, and it would self-assemble to form assemblies. The sample for transmission electron microscopy (TEM) measurement was prepared by dropping the solution onto a copper grid without staining. The grid was then air-dried.

1.3 Apparatus. ¹H NMR data were recorded on a Bruker AV400 spectrometer. UV-Vis spectra were recorded in a quartz cell (light path 10 mm) on a Cary 100 UV-Vis

spectrophotometer equipped with a Cary dual cell peltier accessory. Fluorescence measurements were recorded in a conventional quartz cell (light path 10 mm) on Cary Eclipse and PerkinElmer FL6500. The TEM sample was examined by a TEM (HITACHI HT7700 Exalens). The sample solutions for dynamic light scattering (DLS) measurements were examined on a laser light scattering spectrometer (NanoBrook 173plus and Brookhaven ZetaPals/BI-200SM). Fluorescence microscopy images were observed by a NIKON A1R+ confocal laser scanning microscope (CLSM).

1.4 Data analyses of fluorescence titrations. Fluorescence titrations of LacAC4A were performed in PBS (10 mM, pH = 7.4). The complexations of LacAC4A with reporter dye (RhB and CY5-DM) and DOX were measured by direct fluorescence titrations. A mixed solution containing known amounts of LacAC4A and guest was sequentially injected into 2.5 mL guest solution in a quartz cuvette. The dye concentrations in mixed solution and cuvette are the same to keep dye concentration constant in the course of titrations. The fluorescence intensity was measured ($\lambda_{\text{ex}} = 554$ nm for RhB) before the first addition and after every addition until a plateau was reached. By fitting the fluorescence intensity ($\lambda_{\text{em}} = 575$ nm for RhB) according to a 1:1 host-guest binding stoichiometry, the association constant was obtained.³ The fitting of data from direct titrations was performed in a nonlinear manner, and the fitting modules were downloaded from the website of Prof. Nau's group (<http://www.jacobs-university.de/ses/wnau>) under the column of "Fitting Functions".

1.5 Fluorescence responses of DOX@LacAC4A and CY5-DM@LacAC4A upon the addition of various biologically coexisting species. Various biological coexisting species of blood were added separately to DOX@LacAC4A (10/10 μM) or CY5-DM@LacAC4A (10/10 μM) in PBS (10 mM, pH = 7.4) at 25 °C and stirred for 30 min to monitor the fluorescence intensity of DOX/CY5-DM. The fluorescence of DOX/CY5-DM alone were used as control. The biological coexisting species and their concentration used in these experiments were: NAD 24 μM , BSA 10 $\mu\text{g mL}^{-1}$, glutathione 8.0 μM , urea 4.0 mM, ATP 0.4 μM , glucose 5.0 mM, creatinine 80 μM ,

glutamine 0.5 mM, alanine 0.4 mM, glycine 0.3 mM, arginine 0.14 mM, valine 0.2 mM, lysine 0.2 mM, proline 0.2 mM, K^+ 4.5 mM, Ca^{2+} 2.5 mM, Na^+ 144 mM and Mg^{2+} 0.8 mM. The concentrations of all above components refer to their concentrations in human blood.⁴

1.6 Cytotoxicity Assays *in vitro*. The cytotoxicity of SAC4A, LacAC4A, DOX, DOX@SAC4A and DOX@LacAC4A were determined by measuring the cell viabilities after exposing the cells to these samples. Briefly, cells (Hela and HepG2) were seeded into 96-well plates at a density of 1×10^4 cells/well and grown to 70–80 % confluence, followed by replacing the culture medium with the fresh ones containing SAC4A (1.0, 5.0, 10, 20, 40, 80, 160 μ M), LacAC4A (1.0, 5.0, 10, 20, 40, 80, 160 μ M), DOX (0.5, 1.0, 2.0, 4.0, 8.0, 16 μ M), DOX@SAC4A (0.5, 1.0, 2.0, 4.0, 8.0, 16 μ M) and DOX@LacAC4A (0.5, 1.0, 2.0, 4.0, 8.0, 16 μ M). A humidified atmosphere containing 5% CO_2 was used as normoxic cell culture environment. The hypoxic cell culture environment was adjusted by purging gas mixture (94% N_2 , 5% CO_2 , 1% O_2). After incubating for 4 h under normoxic conditions, the culture medium was replaced with fresh medium. And then, the cells were incubated at 37 °C for 36 h under normoxic and hypoxic conditions, respectively. PBS was used as the negative control. CCK-8 was mixed with culture medium at a volume ratio of 1:9 (freshly prepared) to afford CCK-8 working solution. After the incubation, the cells were rinsed twice with PBS, followed by the addition of 100 μ L CCK-8 working solution and another 1.5 h's incubation. Quantification of the cell viability was achieved by measuring the absorbance with Tecan's Infinite M200 microplate reader ($\lambda_{ex} = 450$ nm). The lactose interference assay was similarly conducted. After DOX, DOX@SAC4A and DOX@LacAC4A with/without lactose (5.0 mM) treatment with HepG2 cells, the cell viabilities of different groups were evaluated under normoxic and hypoxic conditions, respectively.

1.7 Cellular internalization analysis. HepG2 cells (1×10^5 cells per well) were seeded and cultured in confocal imaging chambers. After adherence, the cells were treated with DOX (8.0 μ M) and DOX@LacAC4A (8.0/16 μ M). After incubating for 4 h under

normoxic conditions, the culture medium was replaced with fresh medium. And then, the cells were incubated at 37 °C for 18 h under normoxic and hypoxic conditions, respectively. Cells were washed three times with PBS before imaging by CLSM. The lactose interference assay was similarly conducted. After DOX (10 μM) and DOX@LacAC4A (10/20 μM) with/without lactose (5.0 mM) treatment with HepG2 cells, the cell fluorescence of different groups was evaluated under hypoxic conditions.

1.8 *In vivo* fluorescence imaging. For the animal and the tumor model, male BALB/c nude mice at 6 – 8 weeks were purchased from Vital River Laboratory Animal Technology (Beijing, China). Ethics statement animal procedures were performed in accordance with the recommendations in the Guide for the Care and Use of Laboratory Animals by the National Institutes of Health. The animal study was approved by the Institutional Animal Care and Use Committees of Hebei University (Approval number IACUC-2021011SM).

To establish the xenograft H22 tumor-bearing mouse model, 5×10^6 H22 cancer cells were injected subcutaneously into the right hind leg of BALB/c nude mice. The mice with tumor volumes at around 200 mm³ were randomized into three groups and intravenously injected with 200 μL of CY5-DM (200 μM), CY5-DM@SAC4A (200/200 μM) and CY5-DM@LacAC4A (200/200 μM) with a dosage of 1.0 mg CY5-DM per kg body weight. Then the mice were anesthetized and imaged via an IVIS Lumina imaging system at 1, 3, 8 and 24 h post-injection. For the *ex vivo* study, the mice were sacrificed after 1 h, and the tumor as well as major organs (spleen, kidney, lung, liver, heart and intestine) were collected and subjected for *ex vivo* imaging. Fluorescent images were analyzed.

1.9 *In vivo* antitumor efficacy study. To investigate the antitumor efficiency of DOX@LacAC4A, 5×10^6 H22 cancer cells were injected subcutaneously into the back of the mice. The mice with tumor volumes at around 150 mm³ were randomized into six groups and intravenously injected with PBS (10 mM/200 μL), SAC4A (862 μM/200 μL per dose, 10.8 mg kg⁻¹), LacAC4A (1000 μM/200 μL per dose, 28.2 mg kg⁻¹), DOX

(862 μM /200 μL per dose, 5.0 mg kg^{-1}),^{5, 6} DOX@SAC4A (862/862 μM /200 μL per dose, 5.0/10.8 mg kg^{-1}) and DOX@LacAC4A (862/1000 μM /200 μL per dose, 5.0/28.2 mg kg^{-1}) every two days and continuously monitoring the tumor volumes for 8 days. Tumors were measured by using a vernier calipers and the volume (V) was calculated to be $V = d^2 \times D/2$, where d is the shortest and the D is longest diameter of the tumor in mm respectively. To assess potential toxicities, mice were monitored for weight loss. Animals were euthanized when exhibiting signs of impaired health or when the volume of the tumor may exceed 2000 mm^3 . Tumors were collected for H&E analysis and immunofluorescence staining.

1.10 Statistical analysis. Each experiment was set to three or five groups in parallel, and all data were expressed as mean \pm standard deviation (s.d.). One-way analysis of variance (ANOVA) and Tukey's post-test were used to analyze the significant differences in the data for each group. Statistical significance was denoted as follows: * $p < 0.05$, ** $p < 0.01$, and *** $p < 0.001$.

2 Syntheses of LacAC4A

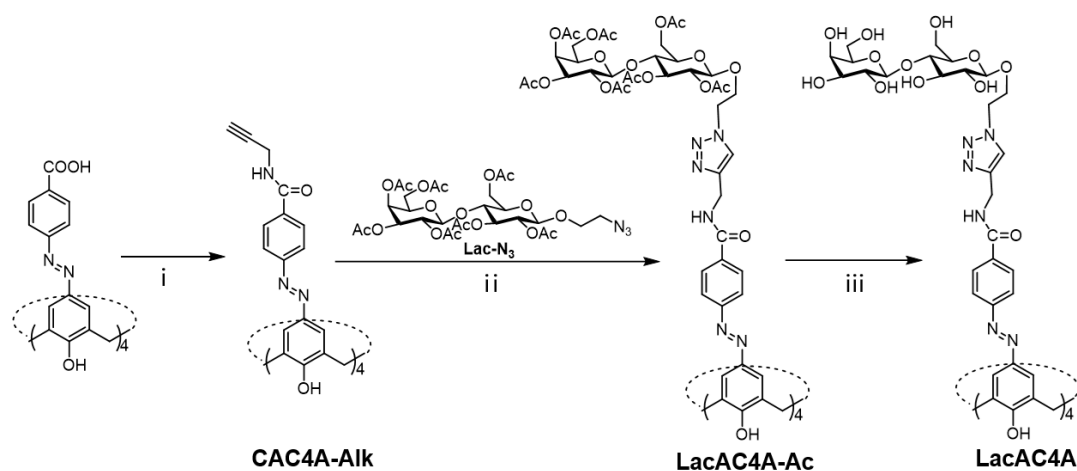


Figure S1. The synthetic route of LacAC4A. (i) Propargylamine, HATU, DIPEA, DMF, rt; (ii) Lac-N₃, THF/H₂O, CuSO₄·5H₂O, L-ascorbic acid sodium salt, 55 °C; (iii) CH₃OH, CH₃ONa, rt.

CAC4A-Alk: In a round bottom flask, CAC4A (250 mg, 0.250 mmol) and HATU (750

mg, 2.00 mmol) were added to 30 mL of DMF, and the reaction was placed in an ice-water bath and stirred for 30 minutes. Propargylamine (0.10 mL, 1.60 mmol) and DIPEA (0.50 mL, 3.00 mmol) were added to the reaction, react for 15 minutes under ice bath condition, and react for 6 h at room temperature. After the reaction was completed, a large amount of water was added until a large amount of precipitate was precipitated. Then the solid was obtained by suction filtration, and the purified product was obtained after drying. CAC4A-Alk (300 mg) was obtained with a yield of 95.0%. ^1H NMR (400 MHz, $\text{DMSO-}d_6$) δ 9.03 (t, $J = 4.7$ Hz, 4H, Ar-OH), 7.96 (d, 8H, $J = 8.4$ Hz, Ar-H), 7.81 (d, 8H, $J = 9.6$ Hz, Ar-H), 7.80 (s, 8H, calix-Ar-H), 4.42 (d, 4H, $J = 12.0$ Hz, calix- CH_2 -H), 4.05-4.04 (m, 8H, Ar- CH_2 -H), 3.68 (d, 4H, $J = 12.0$ Hz, calix- CH_2 -H), 3.11 (t, $J = 2.4$ Hz, 4H, Ar- CH_2 - $\text{C}\equiv\text{CH}$) ppm.

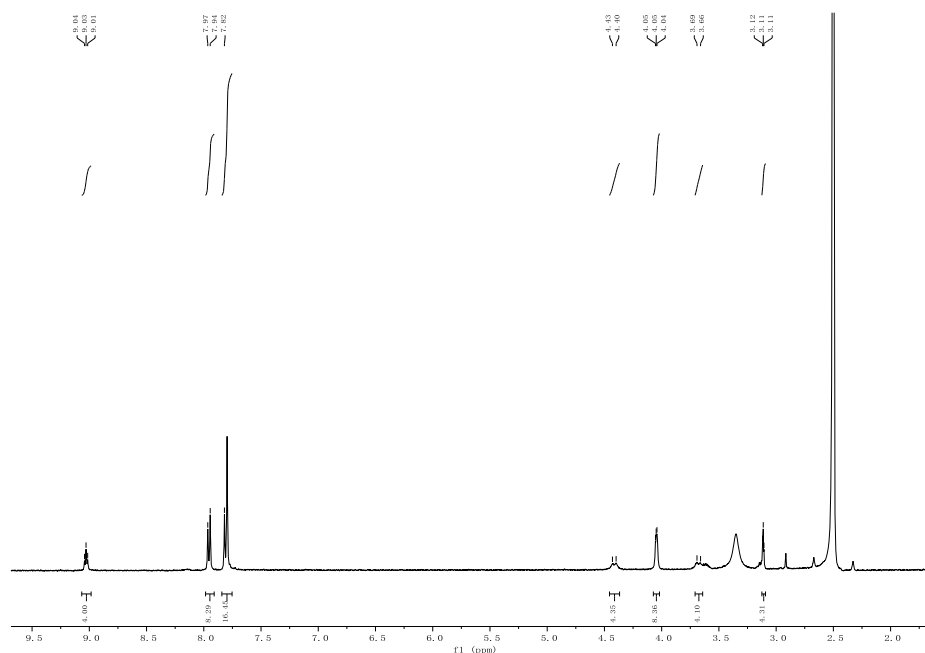


Figure S2. ^1H NMR spectrum of CAC4A-Alk in $\text{DMSO-}d_6$, 400 MHz, 25 °C.

LacAC4A-Ac: Add CAC4A-Alk (200 mg, 0.160 mmol) and Lac- N_3 (540 mg, 0.770 mmol) to 30 mL of THF in a round bottom flask. Then, a water solution of $\text{CuSO}_4 \cdot 5\text{H}_2\text{O}$ (94.0 mg, 0.380 mmol) and sodium ascorbate (76.0 mg, 0.380 mmol) was added. The reaction mixture was stirred for 10 h at 55 °C under N_2 atmosphere. The reaction solvents were evaporated under vacuum. The residue was resolved by CH_2Cl_2 and purified by silica-gel column chromatography using $\text{CH}_2\text{Cl}_2/\text{CH}_3\text{OH}$ (v/v, 30/1) as the

eluent. LacAC4A (400 mg) was obtained with a yield of 65.0%.

^1H NMR (400 MHz, $\text{DMSO}-d_6$ δ): 9.15-9.12 (m, 4H, Triazole-NH), 7.98 (d, 8H, $J = 8.0$ Hz, Ar-H), 7.87 (s, 4H, Triazole-H), 7.81 (d, 8H, $J = 8.0$ Hz, Ar-H), 7.80 (s, 8H, calix-Ar-H), 5.22 (d, 4H, $J = 3.6$ Hz), 5.18-5.14 (m, 4H), 5.10 (t, 4H, $J = 9.2$ Hz), 4.86-4.81 (m, 4H), 4.78-4.72 (m, 8H), 4.65-4.61 (m, 4H), 4.50-4.49 (m, 16H), 4.31 (d, 4H, $J = 11.2$ Hz), 4.21 (t, 4H, $J = 6.8$ Hz), 4.07-3.98 (m, 16H), 3.90-3.73 (m, 16H), 3.70-3.64 (m, 4H), 2.09 (s, 12H, Ac-H), 2.07 (s, 12H, Ac-H), 2.00 (s, 12H, Ac-H), 1.99 (s, 12H, Ac-H), 1.95 (s, 12H, Ac-H), 1.90 (s, 12H, Ac-H), 1.87 (s, 12H, Ac-H) ppm.

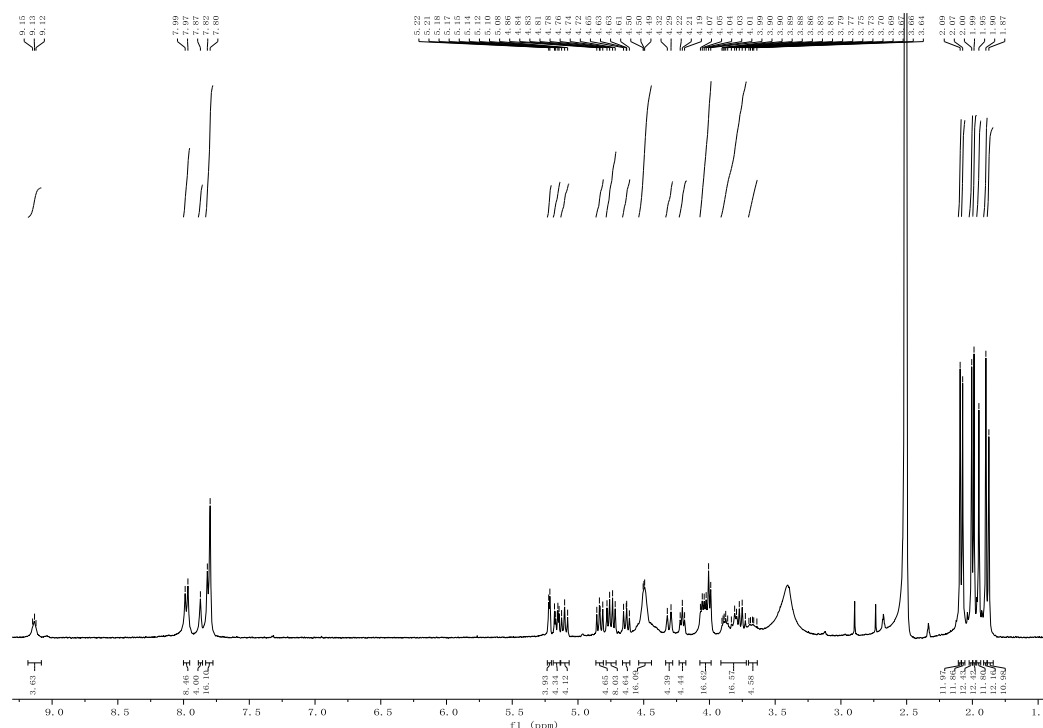


Figure S3. ^1H NMR spectrum of LacAC4A-Ac in $\text{DMSO}-d_6$, 400 MHz, 25 $^{\circ}\text{C}$.

LacAC4A: LacAC4A-Ac (200 mg, 0.0500 mmol) and CH_3ONa (92.0 mg, 1.70 mmol) were dissolved in anhydrous MeOH (20 mL). The reaction mixture was stirred at room temperature for 10 h. The reaction mixture was placed in a cellulose dialysis tube (cutoff 2000) and dialyzed against water for 2 days. The compound LacAC4A (130 mg) was obtained through lyophilization with a yield of 90%.

^1H NMR (400 MHz, $\text{DMSO}-d_6$ δ): 9.12 (t, $J = 5.6$ Hz, 4H, Triazole-NH), 8.04 (s, 4H, Triazole-H), 7.98 (d, 8H, $J = 8.0$ Hz, Ar-H), 7.81 (d, 8H, $J = 8.0$ Hz, Ar-H), 7.80 (s, 8H,

calix-Ar-H), 6.63 (s, 17H, fumaric acid-CH=CH), 5.22 (d, 4H, $J = 4.8$ Hz), 5.11-5.10 (m, 4H), 4.70-4.67 (m, 8H), 4.62-4.50 (m, 28H), 4.3 (d, 4H, $J = 7.6$ Hz), 4.18 (d, 4H, $J = 6.8$ Hz), 4.11-4.05 (m, 8H), 3.94-3.89 (m, 8H), 3.78-3.74 (m, 8H), 3.61-3.60 (m, 8H) ppm. The purity was 96%.

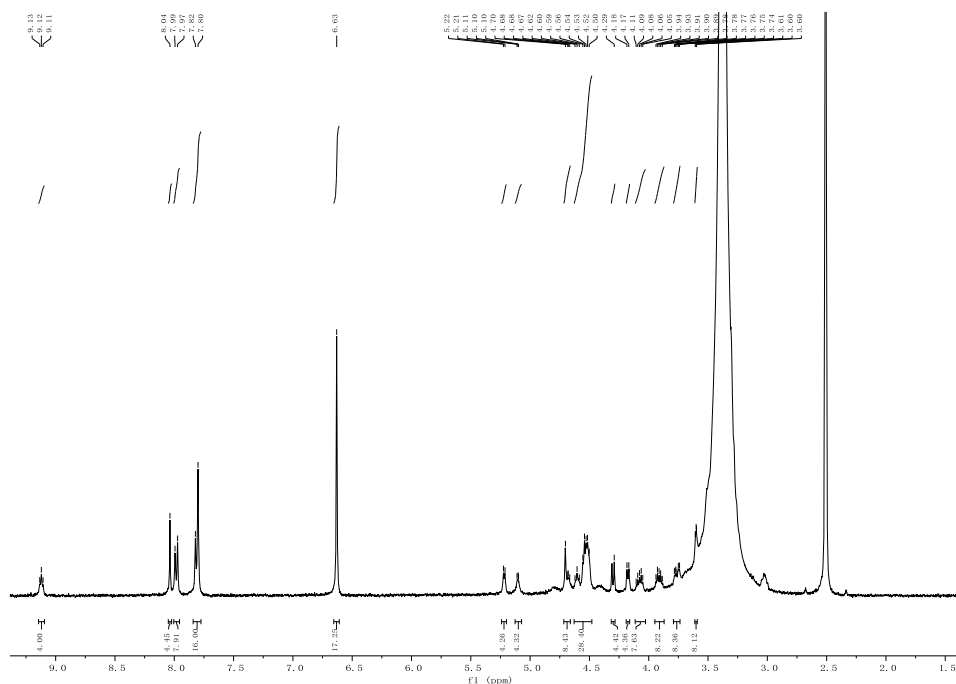


Figure S4. ^1H NMR spectrum of LacAC4A in $\text{DMSO-}d_6$, 400 MHz.

3 Supporting results and experimental raw data

3.1 Job's plot for the complexation of DOX with LacAC4A.

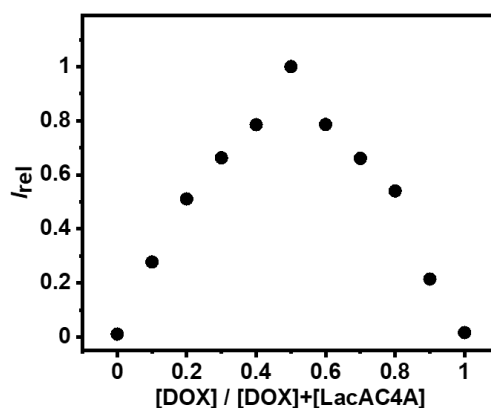


Figure S5. Job's plot for solutions of DOX and LacAC4A, $\lambda_{\text{ex}} = 497$ nm, $\lambda_{\text{em}} = 594$ nm, $[\text{DOX}] + [\text{LacAC4A}] = 1.0$ μM .

3.2 Morphology and stability Evaluation of DOX@LacAC4A.

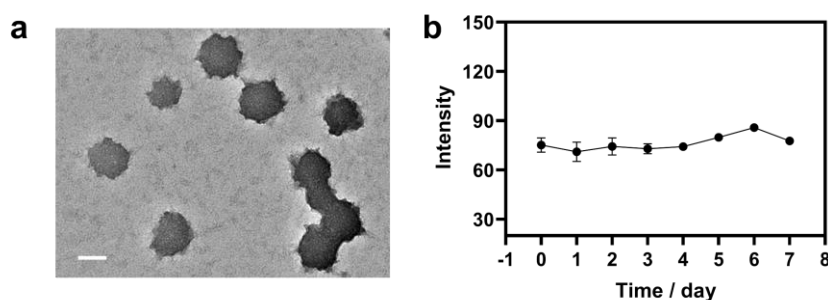


Figure S6. (a) TEM micrograph of DOX@LacAC4A (0.10/0.10 mM). Scale bar, 50 nm. (b) The stability of DOX@LacAC4A (0.10/0.10 mM) in PBS (10 mM, pH = 7.4) at 4 °C by monitoring the size change for 7 days. Data were presented as mean \pm s.d. ($n = 3$).

3.3 The binding affinity of DOX with SAC4A.

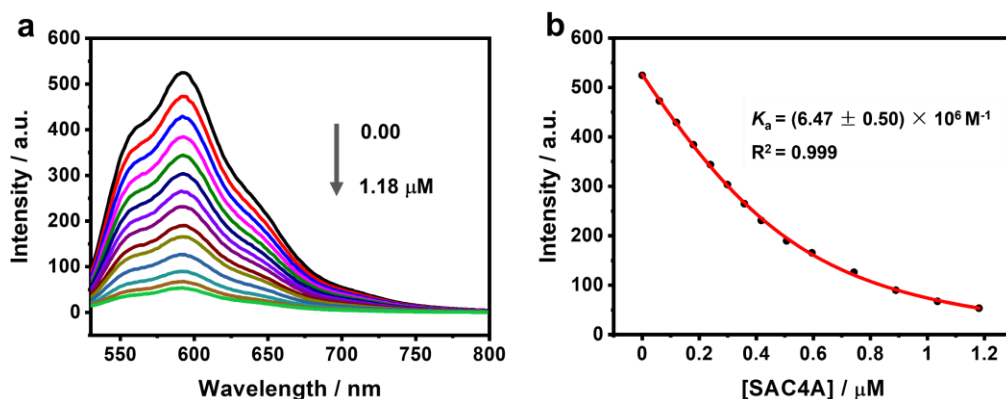


Figure S7. (a) Direct fluorescence titration of DOX (0.50 μ M) with SAC4A (up to 1.2 μ M) in PBS (10 mM, pH = 7.4) at 25°C, $\lambda_{ex} = 497$ nm; (b) The associated titration curve at $\lambda_{em} = 592$ nm was fitted according to a 1:1 binding stoichiometry.

3.4 Cell viabilities of HepG2 cells.

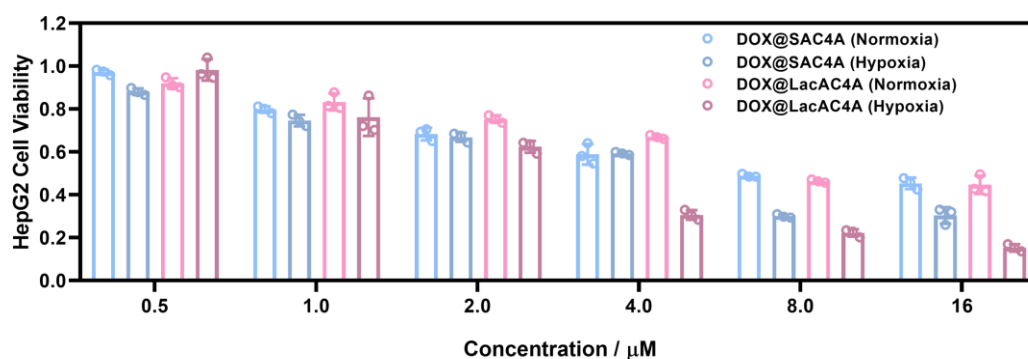


Figure S8. Cell viabilities of HepG2 cells treated with different concentrations of DOX@SAC4A and DOX@LacAC4A under normoxic and hypoxic conditions for 36 h. Data are presented as mean \pm s.d. ($n = 3$).

3.5 Internalization pathway of LacAC4A.

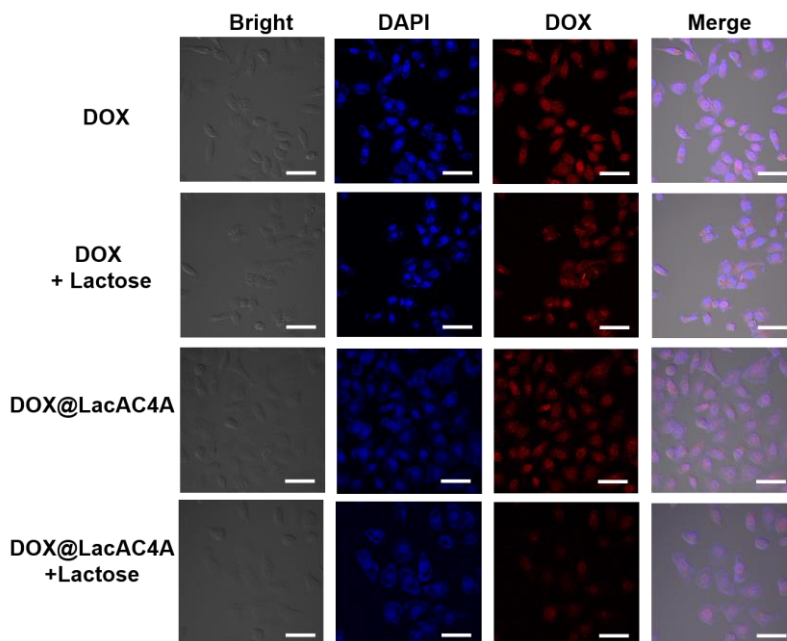


Figure S9. CLSM images of HepG2 cells after treatment with DOX@LacAC4A and DOX with/without lactose under hypoxic conditions and stained by DAPI. Scale bar, 50 μm .

3.6 The binding affinity of CY5-DM with LacAC4A.

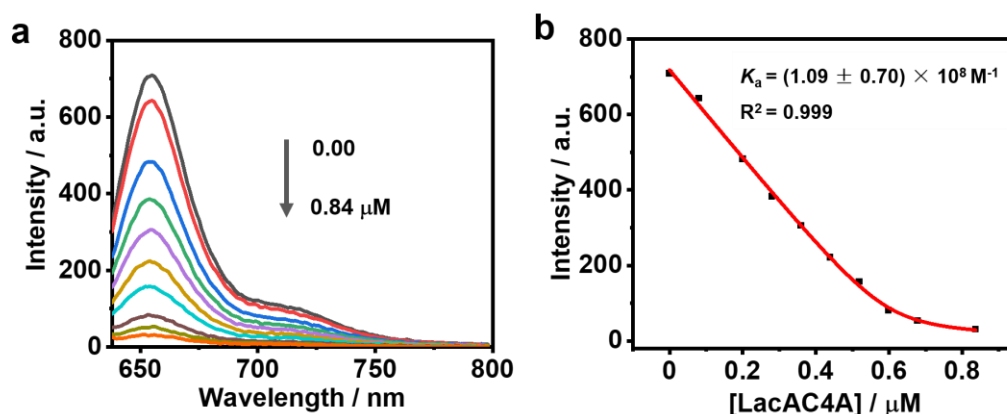


Figure S10. (a) Direct fluorescence titration of CY5-DM (1.0 μM) with LacAC4A (up to 0.84 μM) in PBS (10 mM, pH = 7.4) at 25 $^{\circ}\text{C}$, $\lambda_{\text{ex}} = 635 \text{ nm}$. (b) The associated titration curve at $\lambda_{\text{em}} = 654 \text{ nm}$ was fitted according to the 1:1 binding stoichiometry using the concentration of LacAC4A binding site (one LacAC4A molecular is

considered to have two identical binding sites) to obtain the K_{obs} (observed binding constant).

3.7 Evaluation of the CY5-DM@LacAC4A stability.

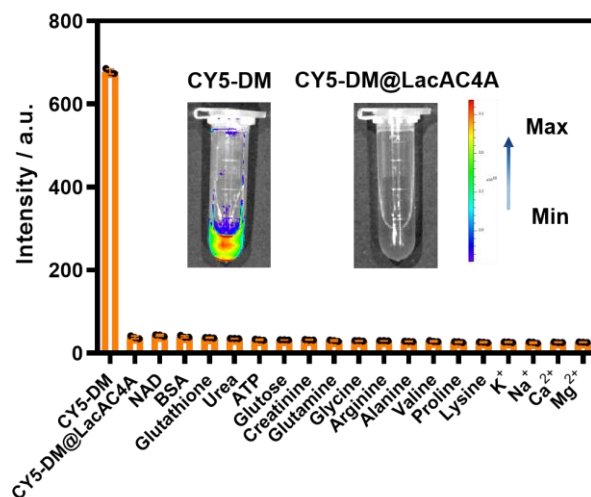


Figure S11. Fluorescent responses of CY5-DM@LacAC4A (10/10 μM) upon the addition of various biologically coexisting species in blood and inset: Fluorescence images of free CY5-DM (10 μM) and CY5-DM@LacAC4A (10/10 μM) in mouse serum.

3.8 *Ex vivo* fluorescence imaging of tumors and major organs.

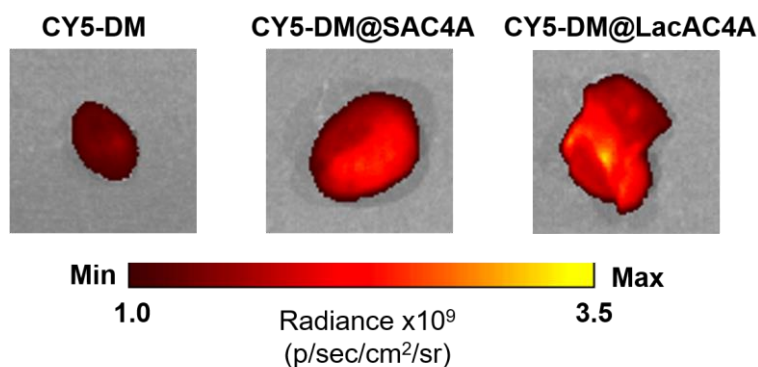


Figure S12. *Ex vivo* imaging of tumors harvested from the euthanized H22-tumor-bearing mice at 1 h post-injection.

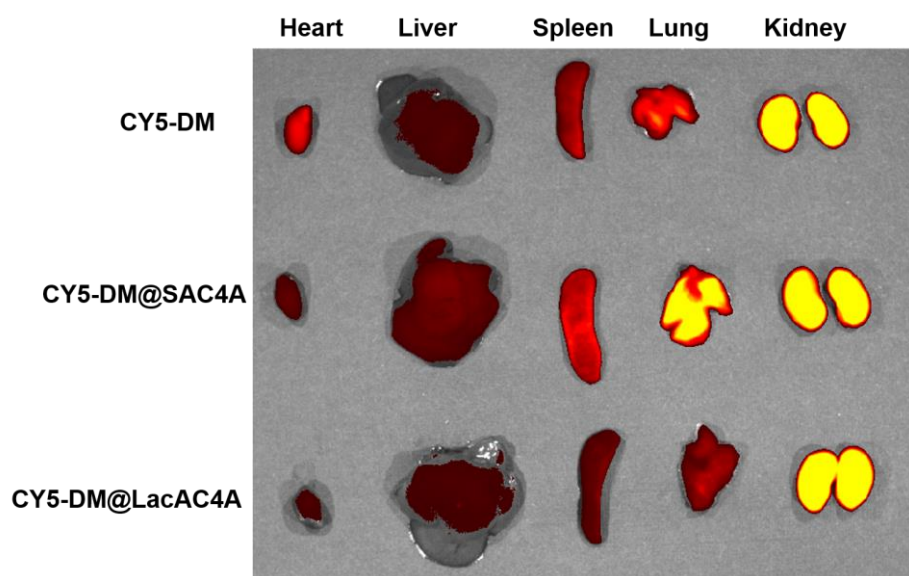


Figure S13. *Ex vivo* imaging of major organs harvested from the euthanized H22-tumor-bearing mice at 1 h post-injection.

3.9 Safety evaluation of supramolecular carrier LacAC4A.

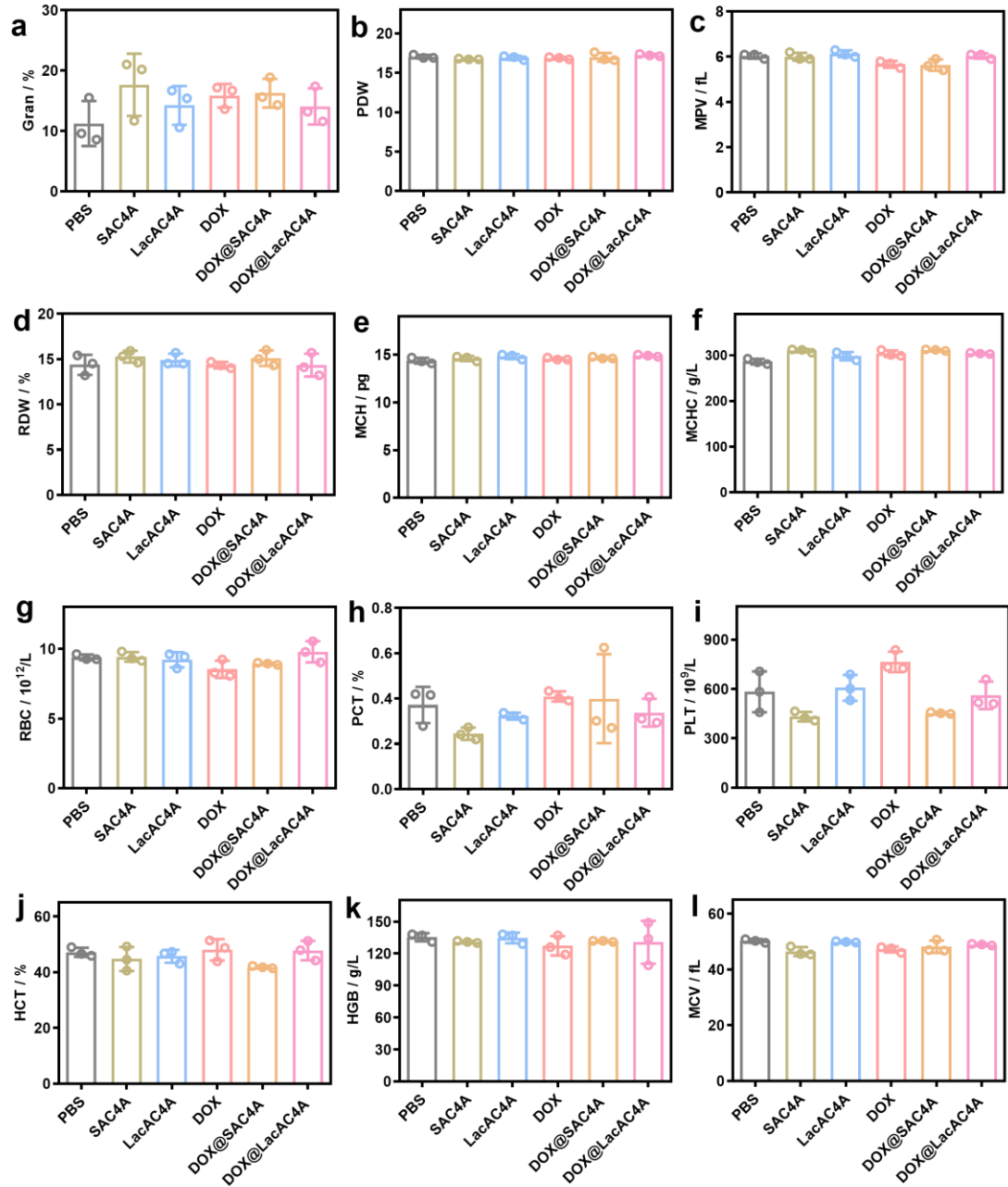


Figure S14. Safety evaluation a–l) Gran (a), PDW (b), MPV (c), RDW (d), MCH (e), MCHC (f), RBC (g), PCT (h), PLT (i), HCT (j), HGB (k), and MCV (l) levels from mice treated with PBS, SAC4A, LacAC4A, DOX, DOX@SAC4A and DOX@LacAC4A.

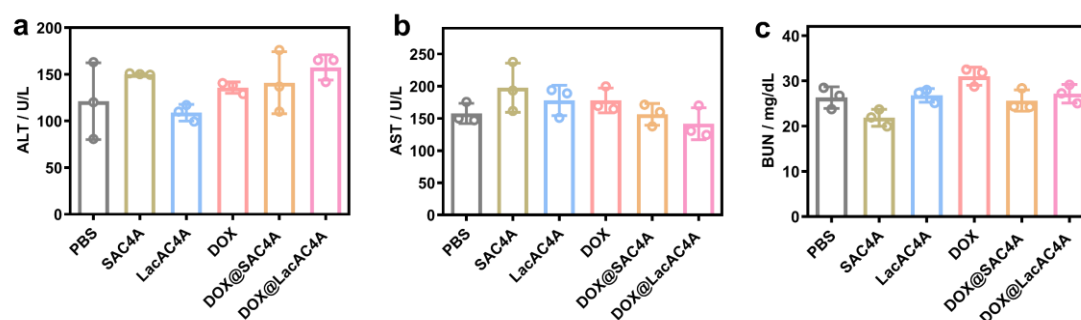


Figure S15. Safety evaluation a–c) ALT (a), AST (b), and BUN (c) levels from mice treated with PBS, SAC4A, LacAC4A, DOX, DOX@SAC4A and DOX@LacAC4A.

3.10 Evaluation of the LacAC4A biocompatibility.

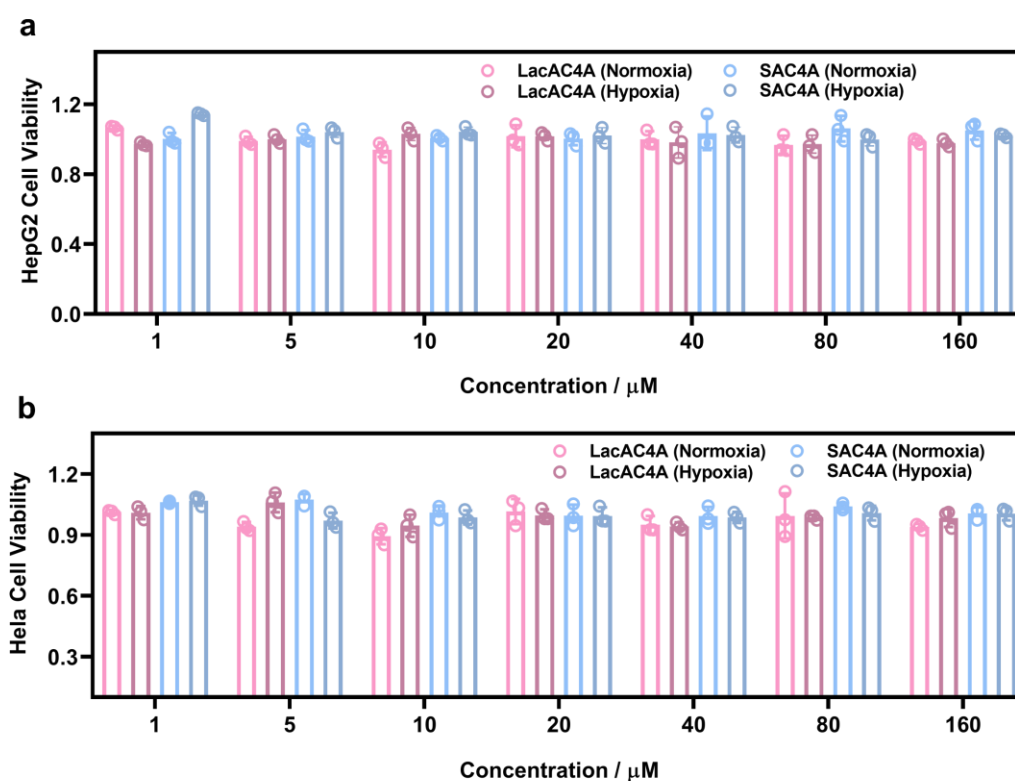


Figure S16. (a) The cytotoxicity of HepG2 cells treated with LacAC4A and SAC4A in different concentrations under normoxic and hypoxic conditions. (b) The cytotoxicity of Hela cells treated with LacAC4A and SAC4A in different concentrations under normoxic and hypoxic conditions. Data was presented as mean \pm s.d. ($n = 3$).

3.11 H&E stains of the major organs.

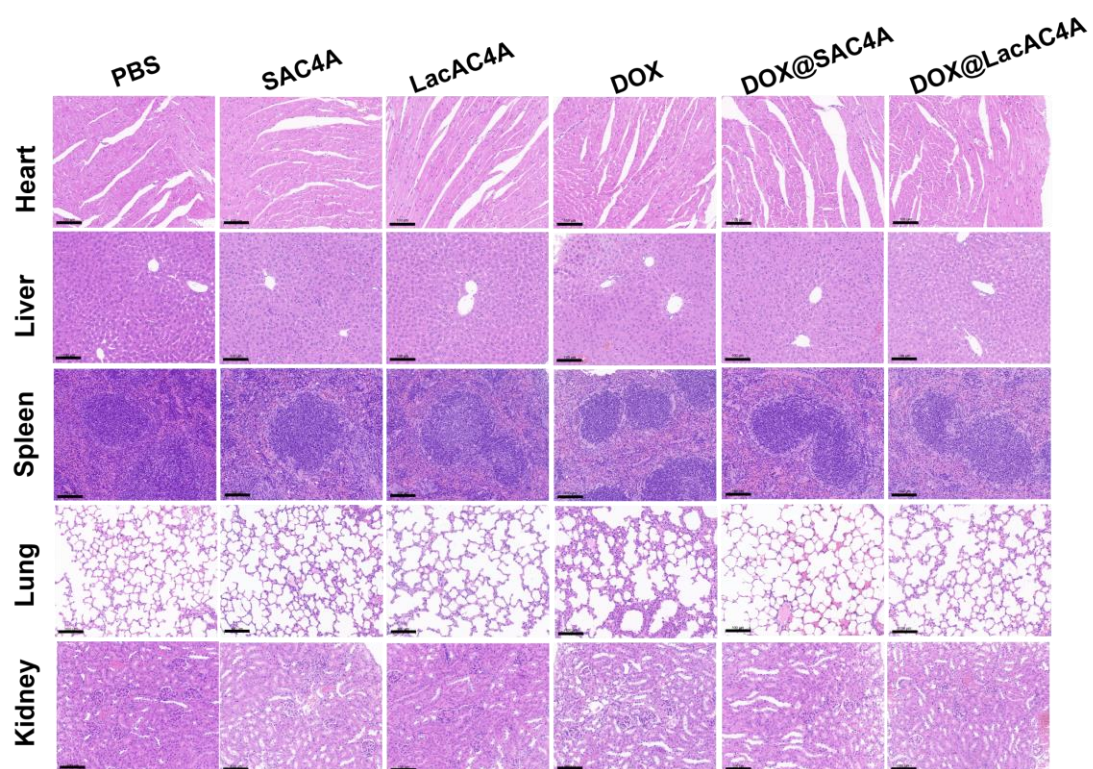


Figure S17. Histological analysis of major organs after different treatments. Scale bar: 100 nm.

4 References

1. T. A. Y. Morita, E. Nomura and H. Taniguchi, *J. Org. Chem.*, 1992, **57**, 3658–3662.
2. W.-C. Geng, S. Jia, Z. Zheng, Z. Li, D. Ding and D.-S. Guo, *Angew. Chem. Int. Ed.*, 2019, **58**, 2377–2381.
3. D.-S. Guo, V. D. Uzunova, X. Su, Y. Liu and W. M. Nau, *Chem. Sci.*, 2011, **2**, 1722–1734.
4. T.-X. Zhang, Z.-Z. Zhang, Y.-X. Yue, X.-Y. Hu, F. Huang, L. Shi, Y. Liu and D.-S. Guo, *Adv. Mater.*, 2020, **32**, 1908435.
5. T. Cheng, J. Liu, J. Ren, F. Huang, H. Ou, Y. Ding, Y. Zhang, R. Ma, Y. An, J. Liu and L. Shi, *Theranostics*, 2016, **6**, 1277–1292.
6. S. Li, X. Jiang, R. Zheng, S. Zuo, L. Zhao, G. Fan, J. Fan, Y. Liao, X. Yu and H. Cheng, *Chem. Commun.*, 2018, **54**, 7983–7986.